

Satellite observations to support monitoring of greenhouse gas emissions

DR STEPHEN HARDWICK AND DR HEATHER GRAVEN

Headlines

- Satellites produce high-resolution global observations of Earth's surface and atmosphere that provide information about greenhouse gas emissions.
- Satellites are used to measure atmospheric concentrations of carbon dioxide and methane. This information is incorporated into atmospheric and statistical models to estimate global and regional sources and sinks of these gases.
- Satellite observations of Earth's surface provide data on land cover, fires, human population and infrastructure, and the biomass and biological activity of vegetation. These data are used to quantify greenhouse gas emissions from land use change and biomass burning, to estimate the spatial distribution of fossil fuel combustion, and to determine flows of greenhouse gases from terrestrial and marine ecosystems.
- National and international initiatives are being coordinated to sustain, advance and share satellite observations.

Aim

The aim of this paper is to provide an overview of the ways in which satellite-based Earth observations can provide information to better understand, estimate and mitigate the emissions of the greenhouse gases carbon dioxide and methane (CO₂ and CH₄). Some key satellite datasets and their applications for studying greenhouse gas emissions are described, separating the observations into two types: measurements of atmospheric concentrations and measurements of Earth's surface. More detailed information on current activities, as well as the potential and planning for future applications, is available from several resources (see Further Information, page 12).

Contents

Headlines	1
Aim	1
Introduction.....	2
Atmospheric CO ₂ , CH ₄ and the global carbon cycle	2
Satellite measurements of atmospheric CO ₂ and CH ₄ concentrations	4
Satellite imaging and spectral analysis of Earth's surface.....	8
Satellite data products and access portals.....	11
Strategies and planning for satellite observations	12
Conclusion	12
References	13

Grantham Briefing Papers analyse climate change and environmental research linked to work at Imperial, setting it in the context of national and international policy and the future research agenda. This paper and other Grantham publications are available from www.imperial.ac.uk/grantham/publications

Introduction

Satellite technology has transformed our ability to observe the state of our planet. Our understanding of the Earth and its key systems has improved significantly since the launch of the first observation satellites in the 1960s. Satellites have the unique ability to provide global coverage of the Earth's surface and atmospheric composition that is not possible using ground-based monitoring techniques. The improvements in weather forecasting and natural resource management that have been made possible by Earth observation satellites have had large socio-economic benefits¹.

Atmospheric concentrations of greenhouse gases have risen sharply in recent decades as a result of human activity. The changes in climate that can be expected as a result of the ongoing emissions of greenhouse gases could have large, harmful impacts on human wellbeing². Consequently, there have been international efforts to reduce greenhouse gas emissions, with many countries setting legally binding targets for reductions over the coming decades.

Greenhouse gas emissions are calculated using standardised bookkeeping approaches based on economic and land management data³. Emission factors relate the economic and land management data, also known as activity data, to the emissions of greenhouse gases, for example the amount of CO₂ released per unit of fuel combusted. Uncertainties in emissions can arise either from the activity data or from the emission

Greenhouse gases

Greenhouse gases absorb infrared radiation emitted by the Earth's surface, atmosphere and clouds that would otherwise be emitted to space. The absorption and re-emission of infrared radiation by greenhouse gases warms the Earth's lower atmosphere and surface, a process known as the "Greenhouse Effect". The accumulation of greenhouse gases emitted by human activities is enhancing the Greenhouse Effect and it is the primary cause of climate change².

The main anthropogenic (human-induced) greenhouse gas emissions are in the form of carbon dioxide, CO₂, which is emitted by fossil fuel combustion, cement production and land use changes including deforestation. Methane, CH₄, is emitted by the extraction and distribution of fossil fuels and by agriculture and waste, in addition to other sources. Other important greenhouse gases include N₂O, emitted mainly through fertiliser use in agriculture, and CFCs (chlorofluorocarbons) and other fluorine-containing gases that have several uses including refrigeration and air conditioning.

factors used, which can often be hard to measure or highly variable in different circumstances. Uncertainties on these "bottom-up" calculations of CO₂ emissions from developed countries are less than 10%^{4,5}. Emissions of CO₂ from developing countries and emissions of other greenhouse gases generally have larger uncertainties. Satellites have the ability to provide activity data for "bottom-up" calculations of greenhouse gas emissions, as well as data to validate emissions estimates.

Atmospheric CO₂, CH₄ and the global carbon cycle

CO₂ and CH₄ are naturally-occurring gases in Earth's atmosphere. CO₂ is produced by plants, animal and bacterial respiration, and is consumed by photosynthesis. A vast amount of CO₂ is dissolved in the oceans and CO₂ is exchanged between the atmosphere and the surface ocean in response to temperature, ocean mixing, and photosynthesis and respiration by marine organisms. Other natural CO₂ exchanges are shown in Figure 1.

The amount of CO₂ produced each year by human activities is a small fraction of the natural exchanges of CO₂ in the global carbon cycle, but anthropogenic CO₂ emissions are perturbing the natural balance of CO₂ and causing its atmospheric concentration to rise (Figure 2). Not all of the emitted CO₂ is accumulating in the atmosphere, however. Approximately half accumulates in the ocean and in terrestrial ecosystems.

CH₄ is produced by wetlands, animals, wildfires and geological seeps, as well as human activities involving fossil fuels, agriculture and waste. The amount of CH₄ produced each year by human activities is roughly equivalent to the amount produced by natural processes. Atmospheric CH₄ is removed primarily by chemical oxidation.

Ground-based measurements of atmospheric CO₂ and CH₄ concentrations began in the 1950s and 1970s, and measurement networks have since expanded to include over a hundred sites around the globe (Figure 2). The observations show increasing trends in concentration of about 0.5 % per year and spatial gradients relating to sources and sinks of CO₂ and CH₄. Both gases have higher concentrations in the northern hemisphere because emissions are concentrated in the densely populated regions between 20° and 60°N. The seasonal fluctuations in CO₂ concentration are a result of the uptake of CO₂ during photosynthesis by plants in the northern hemisphere summer and the subsequent release through respiration during the winter. Concentrations of CH₄ are low in the summer because chemical reactions destroy CH₄ more rapidly in summer.

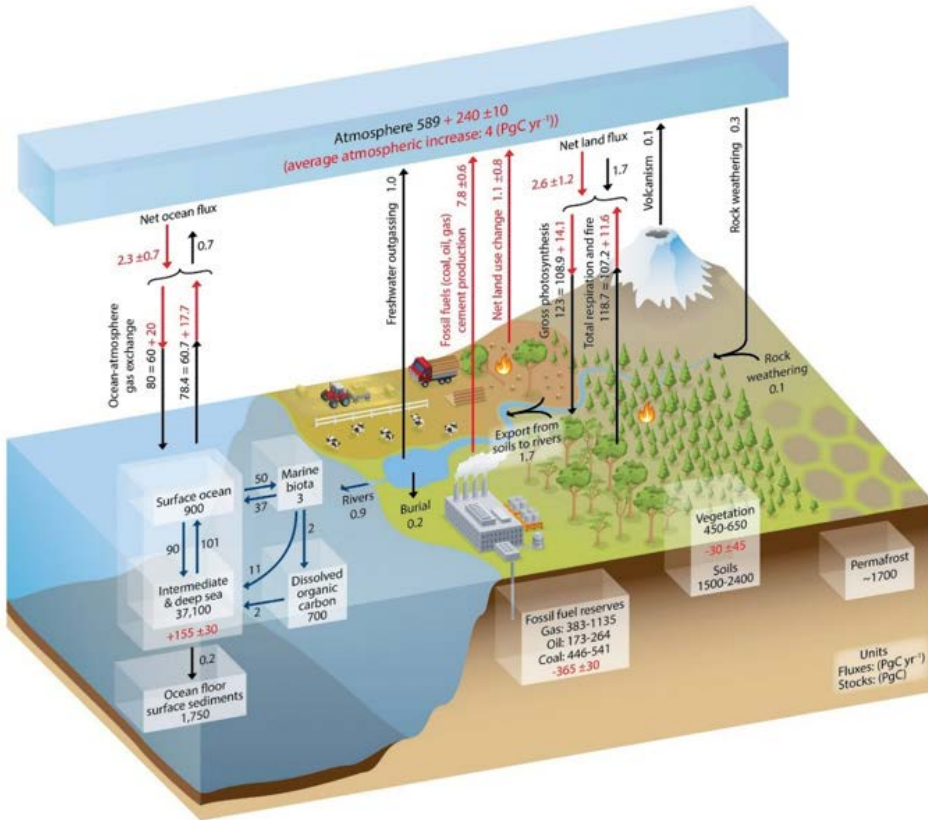


Figure 1: Schematic of the global carbon cycle. Numbers represent the carbon stocks in each reservoir and the annual carbon exchange flows in units of PgC and PgC per year. One PgC is one billion tonnes of carbon. Black numbers are estimates of the natural carbon cycle, prior to the Industrial Era, and red numbers indicate anthropogenic (human-induced) flows and stocks averaged over 2000-2009. Taken from IPCC, 2013².

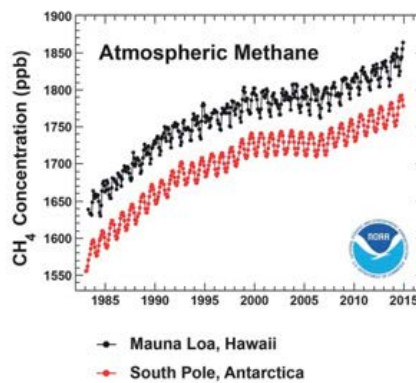
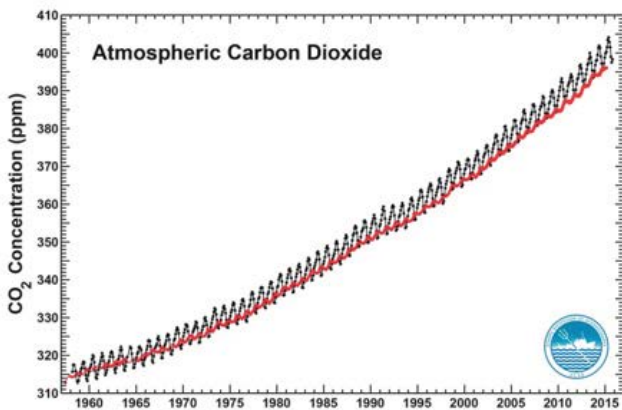


Figure 2: Top: Atmospheric observations of CO₂ and CH₄ at Mauna Loa and the South Pole. Credit: NOAA and Scripps CO₂ Program. Bottom: Map of ground-based measurement sites contributing to the World Meteorological Organization’s World Data Centre for Greenhouse Gases. Credit: JMA.

Satellite measurements of atmospheric CO₂ and CH₄ concentrations

Compared to ground-based measurements, the key advantage of satellite-based measurements is their ability to provide global coverage. Satellite measurements derive atmospheric concentrations of gases using the properties of gases to absorb electromagnetic radiation at specific wavelengths. These instruments primarily use solar radiation that is reflected off the Earth's surface, but some can use radiation emitted by the Earth or from lasers on-board the satellite. An instrument that measures radiation at specific wavelengths is known as a spectrometer.

Satellite-based spectrometers use several wavelengths to measure CO₂ and CH₄ according to their absorption spectra (Figure 3). Satellites that observe shorter near infrared wavelengths are sensitive to CO₂ concentrations near the surface and, therefore, these have proved most useful for investigating surface emissions⁶. Other satellites have been used to detect CO₂ concentrations in the mid-troposphere approximately 6 to 11 km above the Earth's surface using longer thermal infrared wavelengths (e.g. AIRS and IASI satellites).

Detection of column-averaged CO₂, the average concentration of CO₂ within a vertical column from Earth's surface to the top of the atmosphere, relies on measuring absorption in three near infrared wavelength bands. These bands are the weak and strong CO₂ absorption bands in the vicinity of 1.58 and 2.06 μm , respectively, and the molecular oxygen (O₂) A-band in the vicinity of 0.76 μm ⁷. Absorption at the weak CO₂ band at 1.58 μm allows the column-averaged CO₂ to be measured because there is very little absorption by other atmospheric gases at this wavelength. However, absorption can also be affected by variations in surface pressure due to topography or local weather conditions, or by clouds or aerosols.

To account for variations in absorption due to surface pressure and to detect clouds, absorption spectra at the O₂ A-band at 0.76 μm are used. Atmospheric O₂ concentrations are constant and, therefore, absorption spectra in the O₂ A-band can be used to derive the surface pressure and the effects of scattering by clouds and aerosols. Observations at the strong absorption band of CO₂ at 2.06 μm are used to further constrain the impacts of aerosols on estimates of full column CO₂, as absorption in this band is very sensitive to the presence of aerosols. Observations of the column CH₄ concentration are made using the same principles as those of CO₂. Measurements are made based upon CH₄ absorption of wavelengths in the vicinity of 1.67 μm .

Generally, only cloud-free observations can be used to make atmospheric concentration measurements of CO₂ and CH₄. Satellites that are designed to measure atmospheric greenhouse gas concentrations make simultaneous measurements of clouds in conjunction with the CO₂ and CH₄ spectrometer to allow observations affected by clouds to be flagged and discarded. Therefore, frequently clouded regions such as the tropics tend to have poorer coverage.

In nadir viewing mode, the instrument is pointed downwards towards the surface, measuring absorption of reflected sunlight in the atmospheric column directly below the satellite. Because the measurements rely on reflected sunlight, nadir measurements are not possible over dark surfaces, such as the ocean. An alternate viewing mode can be used, glint mode, in which the instrument is angled to point at the bright glint spot on the Earth's surface where specular reflection of solar radiation occurs. The use of reflected sunlight also means that observations cannot be made at night-time or at high latitudes during the winter months.

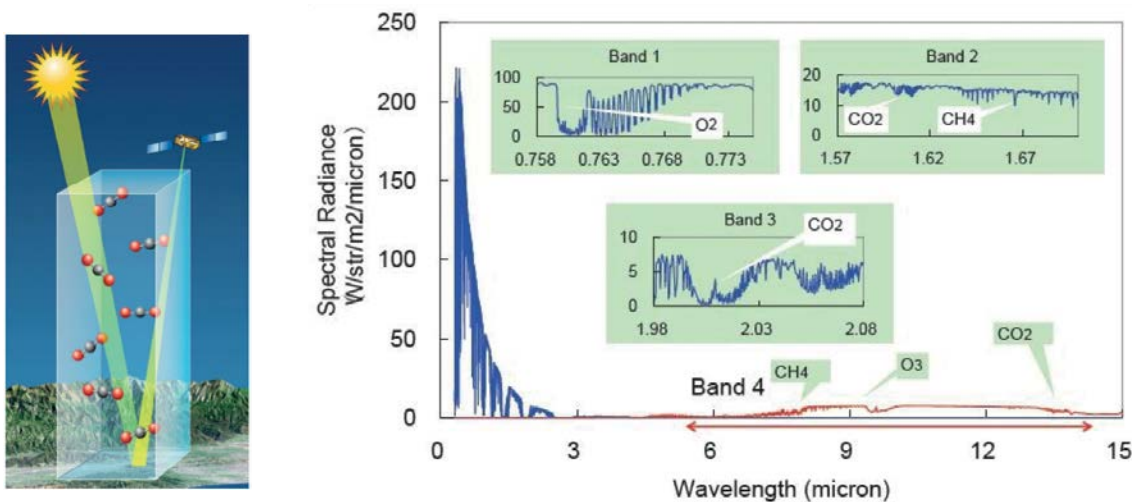


Figure 3: Left: An illustration of satellite detection of reflected solar radiation by the OCO-2 satellite. The intensity of the detected radiation at different wavelengths depends on the abundance of different gases within the portion of the atmosphere traversed by the radiation. Credit: NASA/JPL. Right: Absorption lines observed by GOSAT to determine column-averaged concentrations of CO₂ and CH₄. Inset panels show spectral bands of GOSAT with expanded wavelength axis; the red arrow indicates the wavelength range of Band 4. Credit: JAXA.

Current satellites measuring CO₂ and CH₄ use orbits at around 600 km altitude that pass close to the Earth's poles. As the Earth rotates beneath the satellite, each pass the satellite makes over the surface is displaced in longitude from the previous pass. The width of the Earth's surface observed by the satellite is known as the swath. The footprint refers to the area of an individual measurement within the swath.

Another observational approach uses geostationary satellites, which orbit the Earth at around 36,000 km altitude such that their orbital period is synchronous with Earth's rotation and they remain in constant view of a particular region. Geostationary satellites provide multiple measurements per day and could be particularly useful for observing urban areas⁸.

Calibration and validation

All in situ and remotely sensed data are linked to standard CO₂ concentrations maintained by calibration laboratories⁹. The Total Column Carbon Observing Network (TCCON) is a network of ground-based Fourier Transform Spectrometers that provide accurate measurements of column CO₂, CH₄ and other gases¹⁰. One of the main purposes of TCCON is to validate the observations of satellites¹¹. After a satellite has been launched, its instruments need to be regularly calibrated to ensure they are providing accurate and consistent measurements over the lifetime of the mission. Properties of the instrument can change, and the satellite's orbital characteristics can drift over time. Column readings made at individual TCCON sites have themselves been calibrated using airborne observations of atmospheric composition. Airplanes or balloons are used to directly sample the air at different altitudes, allowing accurate measurements of column averages to be derived¹². While TCCON is very useful for satellite measurements made over land, there is a need for better calibration of measurements made over the ocean¹³.

Current satellite observations of CO₂ and CH₄ concentrations

There have been three satellite missions to measure column-averaged CO₂ and/or CH₄ concentrations: SCIAMACHY, GOSAT and OCO-2. SCIAMACHY ended in 2012, while GOSAT and OCO-2 are currently operating. The missions are briefly summarised below, and their spatial sampling patterns are illustrated in Figure 4.

The Scanning Imaging Absorption Monitoring Spectrometer for Atmospheric Chartography (SCIAMACHY)

SCIAMACHY was launched on board Envisat, a European Space Agency (ESA) satellite which operated from 2002 to 2012. SCIAMACHY provided the earliest record of total column CO₂ and CH₄ measurements with precision of 2-5 ppm in CO₂ and 30-50 ppb in CH₄, with a spatial resolution of 30 x 60 km²¹⁴. SCIAMACHY had a swath width of 960 km and in standard operation it achieved full global coverage in nadir viewing mode every six days.

The Greenhouse Gases Observing Satellite (GOSAT)

GOSAT is operated by the Japanese Aerospace Exploration Agency (JAXA), the Japanese Ministry of the Environment (MOE) and the National Institute for Environmental Studies (NIES). Launched in January 2009, GOSAT was the first satellite dedicated to the monitoring of greenhouse gases in the atmosphere. GOSAT is equipped with a spectrometer (TANSO-FTS) and a cloud and aerosol imager (TANSO-CAI)¹⁵. GOSAT generally records three to five footprints of 10 km diameter across its 700 km swath, achieving global coverage in three days. Measurement precision is 2-3 ppm in CO₂ and approximately 15 ppb in CH₄¹⁶.

The Orbiting Carbon Observatory 2 (OCO-2)

OCO-2 is operated by the US National Aeronautics and Space Administration (NASA) and was launched in July 2014. OCO-2 has a higher precision of approx. 0.5 ppm and high spatial resolution (1 x 1.5 km²), but it has a narrow swath of 10 km. OCO-2 achieves near global coverage every 16 days, however, because of its narrow swath there are areas between its orbital tracks over which measurements are not made (Figure 4). OCO-2 switches between nadir and glint viewing mode. OCO-2 also has a special target mode, in which it focuses its measurement on a specific area, such as a TCCON site.

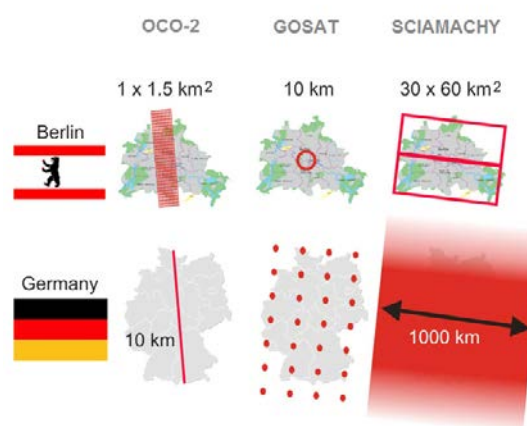


Figure 4: Swath and footprint size of satellites OCO-2, GOSAT and SCIAMACHY, compared to the scale of a city (Berlin) or a country (Germany). Source: Buchwitz et al. 2010¹⁷.

Estimating fluxes based on atmospheric concentrations

The rate of emission or removal of an atmospheric gas is referred to as a flux. Atmospheric concentrations of CO₂ and CH₄ are governed not only by their fluxes, but also by the transport and mixing of air. For example, enhanced CO₂ concentrations are likely to be observed downwind of an area of high CO₂ emissions, but the concentration depends on how rapidly the emissions are mixed with the surrounding air. In order to estimate the spatial distribution and magnitude of CO₂ and CH₄ fluxes using atmospheric concentration measurements, models of atmospheric transport including wind speed and other meteorological data must be included. A method known as a flux inversion is commonly used. The flux inversion calculates a statistical best estimate of the distribution of fluxes, incorporating atmospheric data and models. Because of the use of atmospheric observations, these methods of estimating emissions are referred to as “top-down,” in contrast to the “bottom-up” inventories that use economic and land management data.

Flux inversions frequently use a “first-guess” or *a priori* estimate of the surface fluxes and their uncertainty. These *a priori* fluxes are needed to help constrain the inversion, as uncertainties in both the observed concentrations and the transport model often mean that a single solution to the flux inversion cannot be reached. *A priori* fluxes are derived from bottom-up anthropogenic emission inventories, and from models of terrestrial ecosystem and ocean processes.

Flux inversions for terrestrial ecosystem and ocean CO₂ fluxes

Several studies^{13,18} have used GOSAT data in flux inversions for CO₂ and OCO-2 data is starting to be used in flux inversions. These applications build on previous work using ground-based and aircraft CO₂ data in flux inversions^{19,20}.

Importantly, flux inversions for CO₂ do not presently estimate fossil fuel CO₂ emissions. Fossil fuel CO₂ emissions are assumed to be well-known from emission inventories, and their influence on atmospheric CO₂ concentrations is subtracted from the observations before performing the flux inversion to estimate CO₂ fluxes from the ocean and terrestrial ecosystems. The flux inversions therefore primarily help to evaluate the regional distribution and potential mechanisms for the “CO₂ sink” in the ocean and terrestrial biosphere that is presently sequestering about half of the anthropogenic CO₂ emissions. Understanding these processes is key to predicting future changes in atmospheric CO₂ and ecosystem responses to climate and environmental change. In some cases, these fluxes are also related to human activities through agriculture and forest management. There are, however, large uncertainties associated with satellite-based inverse flux estimates due to the limitations of currently available satellite observations.

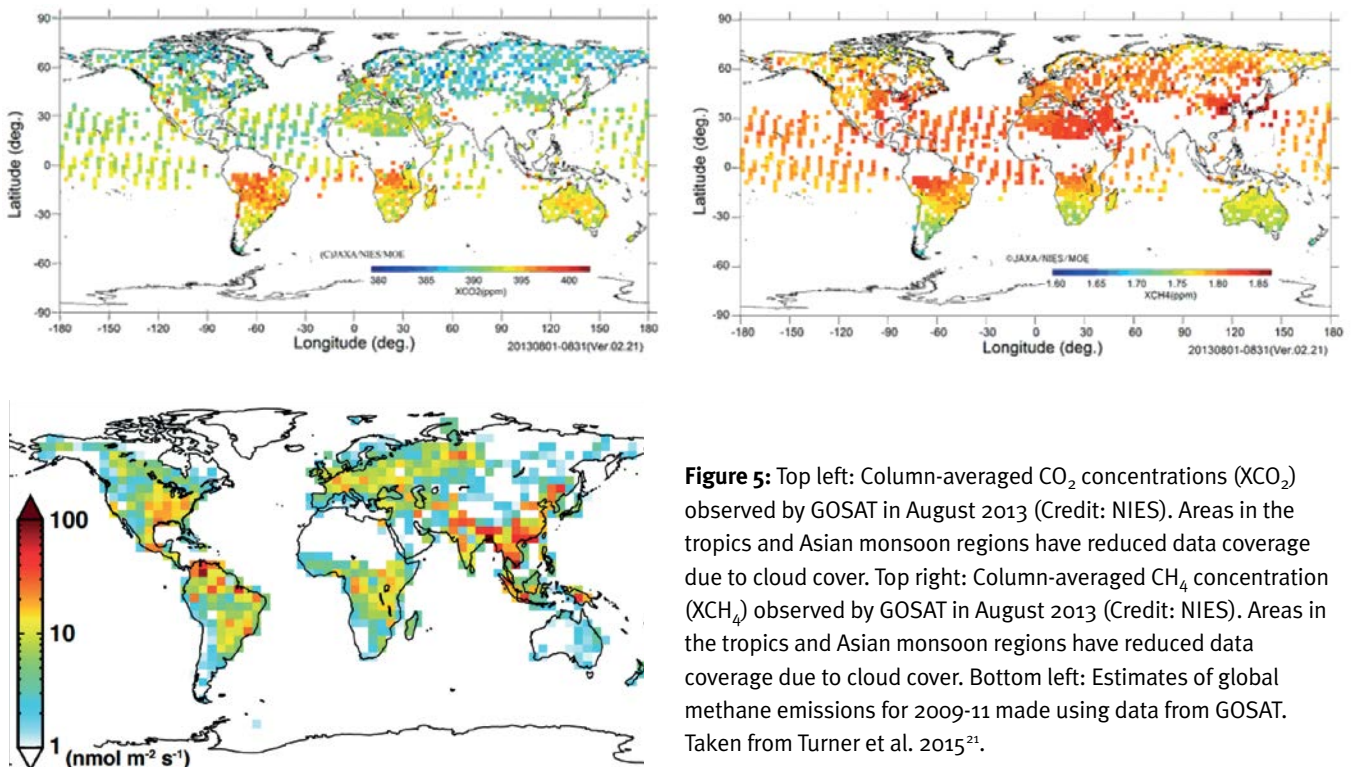


Figure 5: Top left: Column-averaged CO₂ concentrations (XCO₂) observed by GOSAT in August 2013 (Credit: NIES). Areas in the tropics and Asian monsoon regions have reduced data coverage due to cloud cover. Top right: Column-averaged CH₄ concentration (XCH₄) observed by GOSAT in August 2013 (Credit: NIES). Areas in the tropics and Asian monsoon regions have reduced data coverage due to cloud cover. Bottom left: Estimates of global methane emissions for 2009-11 made using data from GOSAT. Taken from Turner et al. 2015²¹.

Potential approaches for estimating fossil fuel CO₂ emissions using satellite CO₂ data

Presently, satellite observations of CO₂ are used in flux inversions to estimate CO₂ exchanges with the ocean and terrestrial ecosystems, but not to estimate fossil fuel CO₂ emissions. This is because the uncertainty in fossil fuel CO₂ emissions is usually much lower than the uncertainty in natural CO₂ fluxes, and atmospheric variations in CO₂ are often dominated by terrestrial ecosystem exchange. Several avenues of research are being developed to focus on high-emission areas or to integrate satellite CO₂ data with other observations.

Targeting megacities and large point sources: Megacities are defined as metropolitan areas with populations exceeding 10 million people. There are currently 28 megacities and they are home to 12.5% of the world's population^{8,22}. Due to the high density of emissions in megacities, column-averaged CO₂ concentrations above megacities are estimated to be enhanced by up to several ppm, depending on the density, topography and emissions of the city⁵. Other strong point sources such as large power plants are also expected to create CO₂ enhancements detectable by satellites²³.

Enhanced CO₂ concentrations have been observed by GOSAT over Los Angeles and Mumbai, compared to rural areas nearby²⁴. These results indicate that changes in emissions of around 20% could be detected by satellite, although cloudy conditions can limit observational coverage in the wet season in regions such as Mumbai. Another observational challenge for some large cities is their high concentrations of aerosols, which interfere with the CO₂ retrieval. Observation of megacities may improve with OCO-2's higher resolution measurements and targeting capabilities, even though OCO-2's narrow swath does not allow regular observation of all megacities.

Tracers of fossil fuel emissions: Combining satellite CO₂ data with complementary observations can help to distinguish CO₂ added by fossil fuel combustion from the effects of natural CO₂ fluxes. For example, carbon monoxide, CO, and nitrogen oxides, NO_x, are produced during fossil fuel combustion and observed by satellite. With knowledge of the emission ratios of CO and NO_x to CO₂ during fossil fuel combustion, the amount of fossil-fuel derived CO₂ can be estimated^{25,26}. This technique is sensitive to variability and uncertainty in the emission ratios of CO and NO_x to CO₂, and to other processes influencing CO and NO_x such as biomass burning and atmospheric chemistry.

Satellite CO₂ data could also be combined with ground-based tracer observations such as radiocarbon (¹⁴C) in CO₂. Radiocarbon is an isotope of carbon that is produced naturally within the atmosphere, but it is not present in million-year-old fossil fuels due to radioactive decay. While radiocarbon cannot be detected by satellites, ground based and airborne observations can quantify fossil fuel-derived CO₂ by measuring the dilution of ¹⁴C in comparison to a reference level²⁷. A targeted network of ¹⁴C observations could help characterise the proportion of fossil fuel CO₂ in certain locations and their diurnal and seasonal cycles⁵. For example, urban networks of ground-based measurements are being developed in Los Angeles and Paris, with plans to expand to other megacities²⁸.

Flux inversions for natural and anthropogenic CH₄ fluxes

In contrast to CO₂, anthropogenic CH₄ fluxes have large uncertainties and strong influences on atmospheric CH₄ variability²⁹. Therefore, atmospheric CH₄ flux inversions are used to estimate both anthropogenic and natural CH₄ fluxes.

Several studies have used CH₄ data from SCIAMACHY and GOSAT to estimate CH₄ fluxes in regional and global studies (e.g. Figure 5). These studies have provided important validation for bottom-up CH₄ emission inventories and wetland models. Studies focusing on North America have found that CH₄ emissions from livestock were higher than estimated by bottom-

up inventories³⁰, and identified a hotspot of emissions in the Four Corners area associated with fossil fuel extraction³¹. Recent work using SCIAMACHY indicates tropical wetland fluxes are stronger and more variable than previous estimates³². Wetlands may contribute an important climate change feedback, as their CH₄ fluxes increase with warmer temperatures and more precipitation.

As with CO₂ flux inversions, there are substantial uncertainties in CH₄ flux estimates due to the limitations of currently available satellite observations. Applications for monitoring CH₄ emissions are similarly limited by the difficulty in discerning natural CH₄ sources from anthropogenic ones, and in discerning anthropogenic CH₄ sources of different types.

Future missions to measure atmospheric CO₂ and CH₄ concentrations

With SCIAMACHY ending in 2012, GOSAT now operating after the end of its nominal life in 2014, and OCO-2's nominal life ending in 2016, the continuation of space-based observations of CO₂ and CH₄ concentrations will require the launch of new satellites. There are a number of missions planned or proposed for the coming years, some of which are described briefly here.

TROPOMI: The Tropospheric Monitoring Instrument (TROPOMI) will be launched in 2016 on board ESA's Sentinel-5P satellite. TROPOMI will provide measurements of column CH₄, CO, NO₂ and other species. TROPOMI will have a very wide swath (2,600 km) and will provide daily global observations with a spatial resolution of 7 x 7 km².

TanSat: TanSat is a Chinese CO₂ observation satellite mission planned for launch in 2016³³. TanSat is planned to have a spatial resolution of 1 x 2 km² and a swath width of 20 km³⁴, similar to OCO-2.

GHGSat: A commercial enterprise to launch a constellation of satellites providing services for oil and gas, power generation, mining and other industries, GHGSat aims to provide column-averaged greenhouse gas concentrations at high spatial resolution of 50 x 50 m² over targeted areas³⁵. Launch of a demonstration satellite is expected in 2016.

GOSAT-2: JAXA's successor to GOSAT is under construction and expected to launch in 2017. GOSAT-2 will provide column-averaged measurements of CO₂ and CH₄, similar to GOSAT, and it features an intelligent pointing system to angle the instrument to observe more cloud-free scenes^{36,37}.

OCO-3: NASA's Orbiting Carbon Observatory 3 (OCO-3) will use the spare instrument from OCO-2 to observe column CO₂ concentrations from the International Space Station, making particular use of "target mode" to focus on regions of high interest. Launch is expected in 2018.

MERLIN: The Methane Remote Sensing Lidar Mission (MERLIN) is a joint mission between the French and German space agencies. MERLIN will observe column CH₄ concentrations using pulsed lasers, allowing measurements to be made at night and during winter at high latitudes. Launch is proposed for 2019.

MicroCarb: A French space agency (CNES) mission that will observe column CO₂ concentrations with a footprint size of 5 x 6 km² and a narrow swath. Launch is planned for 2020.

CarbonSat: This satellite would combine a small footprint size (2 x 2 km²) with a wide swath (500 km) to provide high resolution measurements of column CO₂ and CH₄ with global coverage every 5-6 days^{38,39}. CarbonSat was a candidate mission that was not selected for Earth Explorer 8, but the design may be considered for other missions.

ASCENDS: Active Sensing of CO₂ Emissions over Nights, Days and Seasons (ASCENDS) is a NASA mission under consideration to transmit and detect pulsed lasers to measure column CO₂ concentrations⁴⁰. Launch is not expected until at least 2023.

Satellite imaging and spectral analysis of Earth's surface

Satellite observations of the Earth's surface provide detailed information on land cover, forest biomass, fires, biological productivity, and human energy consumption that can be used to estimate several types of emissions and their spatial distribution.

Land use change

Land use change is the second largest source of anthropogenic greenhouse gas emissions, after fossil fuel combustion². Surface observations made by satellites can be used to monitor deforestation and forest degradation, and to provide estimates of the carbon contained in above-ground biomass that is subject to release by changes in land use.

Satellite images of Earth's surface can be used to create maps of land cover, including forest area. For example, NASA's Landsat programme provides a continuous record of surface imaging from 1972 to the present day using a series of satellite missions. Landsat 8, the most recent continuation of the programme, was launched in 2013, and it is complemented by similar measurements from ESA's Sentinel 2A and 2B (launching in 2015-16) to provide sub-weekly temporal resolution. These satellites observe the visible and near infrared wavelengths and produce high resolution (10-60 m) images of the Earth's surface. Landsat data has recently been used to produce global maps of forest cover change, and to show that net tropical deforestation accelerated by 62% between the 1990s and 2000s^{41,42} (Figure 7).

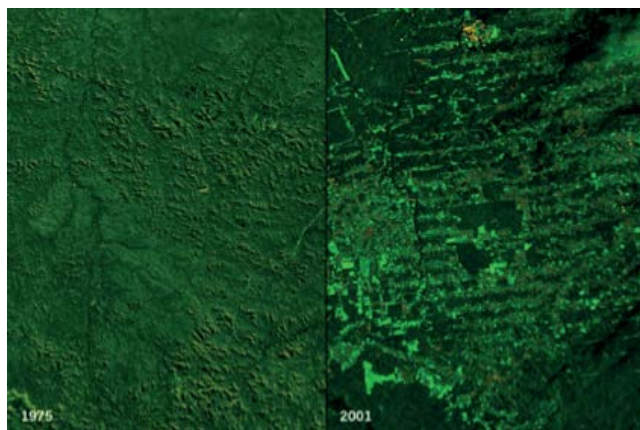


Figure 6: Landsat images of forest in Rondônia in the Brazilian Amazon taken in 1975 and 2001. Credit: Goddard Space Flight Center Visualisation Studio/NASA.

Biomass in forests can be estimated by laser altimetry, which transmits a pulse of laser light down to the Earth's surface and records how long it takes for the reflected light to return to the satellite. Over forests, a fraction of the laser pulse is reflected from the forest canopy, and another fraction is reflected from the ground. Therefore, forest canopy height can be derived from the difference between the distances travelled by light reflected from the canopy top and light reflected from the ground. Topographical data can be used to account for sloped terrain. Tree height can then be related to biomass through relationships developed with in situ forest biomass measurements. Observations from the Ice, Cloud and land Elevation Satellite (ICESat) have been used to estimate the biomass of forests and produce a benchmark map of forest carbon stocks in the tropics^{43,44}.

Several studies have combined remotely sensed deforestation and biomass maps to estimate carbon emissions due to land use change⁴⁵⁻⁴⁷. The uncertainty on these estimates is large (25-50%). However, satellites provide the only way of monitoring forest cover changes over large scales, as ground surveys are too costly and impractical⁴⁶.

Fires

Surface imaging in infrared wavelengths can detect high brightness temperatures that signify actively burning fires⁴⁸ (Figure 7). Several satellites are used for fire 'hotspot' detection, including MODIS, VIIRS, AVHRR, SEVIRI and Landsat⁴⁹⁻⁵². MODIS (Moderate Resolution Imaging Spectroradiometer) has also been used to detect burned areas after a fire has occurred using the differences in reflective properties of burned land compared to vegetation⁵³. Greenhouse gas emissions from fires can be estimated by combining satellite estimates of burned area with estimates of the amount of biomass burned using models⁵⁴. Emissions of CO₂, CH₄ and other trace gases are estimated using typical emission ratios for fires in different forest types.

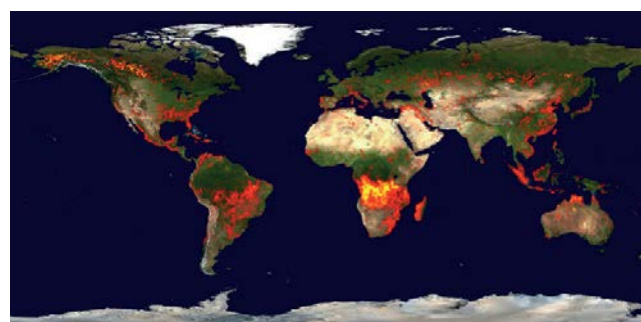


Figure 7: Active fires detected by MODIS for the ten day period from 20 – 29 June 2015 inclusive. Coloured areas indicate the detection of at least one fire during the observation period, ranging from red, indicating a low fire count, to yellow, which indicates a high fire count. Credit: NASA Earthdata.

Night-time lights

Bottom-up inventories of greenhouse gas emissions are typically calculated as national or state totals^{3,55}. To estimate the spatial distribution of emissions, the emissions are allocated according to the locations of cities, power stations, roads, agriculture and other types of human activity.

The spatial distribution of light emitted from the Earth's surface at night (Figure 8) provides a proxy for energy consumption. The US Air Force Defence Meteorological Satellite Project Operational Linescan System (DMSP-OLS) satellites are capable of detecting low-level lights on the Earth's surface. Images of night time lights have been used in conjunction with national inventories of fossil fuel emissions and a directory of known point source emitters, such as power stations and factories, to produce high resolution gridded datasets of fossil fuel CO₂ emission^{56,57}. Gridded emissions data are commonly used in flux inversions, and observations of changing night light distributions can provide information on trends in emissions, including migration and economic shifts⁵⁷.



Figure 8: Night-time lights in Europe and North Africa by Craig Mayhew and Robert Simmon, from data provided by Christopher Elvidge of the NOAA National Geophysical Data Center. [Public domain], via Wikimedia Commons.

Biological productivity

Biological productivity in terrestrial and marine plants can be estimated by observing how much radiation is absorbed by the Earth's surface in the wavelengths associated with photosynthesis (0.4 – 0.7 μm). Locations with dense, active vegetation and high rates of photosynthesis absorb more light, and therefore, less light is reflected to space. Global estimates of the fraction of absorbed photosynthetically active radiation (fAPAR) by terrestrial vegetation have been produced using data from MODIS⁵⁸, AVHRR⁵⁹ and a number of other satellites⁶⁰. A similar product that is widely-used is the Normalized Difference Vegetation Index (NDVI), also known as “greenness”, which compares surface reflectance in the red and near infrared wavelengths (Figure 9). This provides information on the photosynthetic activity of vegetation, as chlorophyll absorbs red light and reflects near infrared light. Chlorophyll contained within phytoplankton in the ocean can be observed using similar methods, providing information on the biological activity of marine ecosystems⁶¹ (Figure 9). Satellite observations have provided unique insight on the response of terrestrial and marine ecosystem productivity to climate variability, for example, through changes in precipitation, temperature and nutrient availability^{62,63}, that can help to understand and predict how ecosystems will respond to future climate change.

Actively photosynthesising plants also re-radiate some solar radiation at wavelengths between 0.68 and 0.8 μm . This solar-induced fluorescence (SIF) can be detected remotely and used to estimate the rate of CO₂ uptake by plants, as well as plants' response to stress. The O₂ A-band at 0.76 μm that is detected by GOSAT and OCO-2 can be used to measure this fluorescence⁶⁴, and the first global space-based measurements were produced in 2011⁶⁵.

Satellite-based estimates of photosynthetic activity are used in models of terrestrial and marine ecosystem CO₂ exchange, with some also incorporating satellite observations of land cover and fire⁵⁴. These models often provide *a priori* flux estimates for flux inversions using atmospheric CO₂ data. The models are also used to investigate ecosystem functioning and the response of ecosystems to land management, climate and environmental changes, providing information on the mechanisms driving the net uptake of CO₂ from the atmosphere.

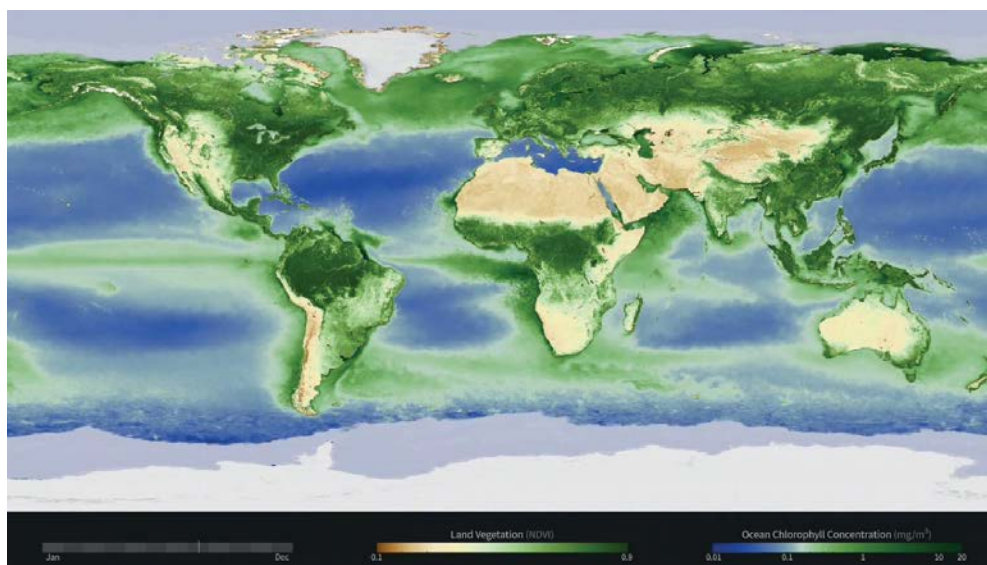


Figure 9: Multi-year mean global Normalized Difference Vegetation Index (NDVI) and Ocean Chlorophyll Concentration derived from observations of multiple satellites for August. Credit: NASA Goddard Space Flight Centre.

Future surface observation missions

Many missions for observing the Earth's surface are currently planned and proposed. Some key missions include:

Landsat 9: Landsat 9 will extend the high-resolution surface imaging datasets that have been produced by NASA since 1972. Landsat 9 is planned for launch in 2023 and will be similar in design to Landsat 8, to ensure continuity in the dataset⁶⁶.

Biomass: Scheduled to be launched by ESA in 2020, Biomass is an active sensor that will use radar to measure the biomass of forests. Biomass will transmit radio waves with a frequency of 435 MHz to measure forest canopy height and vertical structure⁶⁷.

Fluorescence Explorer (FLEX): FLEX is a satellite mission that has been selected by ESA for Earth Explorer 8, launching in 2022. Unlike previous missions where solar induced fluorescence was a secondary objective, FLEX is designed specifically to optimise observations of solar induced fluorescence, using a wide band spectrometer that detects radiation between wavelengths of 500 and 780 nm⁶⁸. FLEX includes other key measurements needed to interpret fluorescence, such as canopy temperature and reflectance.

Satellite data products and access portals

Satellite data is provided free to the public through several access portals. ESA's Earth Online portal provides access to Envisat and Earth Explorer missions (<https://earth.esa.int/>). NASA's Earth data portal (<https://earthdata.nasa.gov>) provides access to all data derived from their satellite missions. JAXA and NIES have created a GOSAT User Interface Gateway (<http://data.gosat.nies.go.jp>).

Several types of data can be provided, which are often referred to as data levels. Typically, Level 1 data includes calibrated spectra and radiances for individual satellite observations. Level 2 data contains the calculated physical quantity of interest, for example, the column-averaged CO₂ concentration for an individual observation. Level 3 data includes gridded or interpolated maps.

Higher level products are also sometimes made available; for example, estimates of regional CO₂ and CH₄ fluxes from a flux inversion using GOSAT data are distributed by JAXA and NIES. The EU's Copernicus programme (<http://www.copernicus.eu/>) aims to develop and provide useful, high level data products to end-users including public authorities, EU bodies, international organisations, NGOs, and the public in an accessible and understandable format. As part of this programme, the Copernicus Climate Change Service will provide consistent estimates of Essential Climate Variables, which include atmospheric concentrations of CO₂ and CH₄. These estimates are supported by the work of the EU's Greenhouse Gas Climate Change Initiative, which aims to provide high quality global datasets of XCO₂ and XCH₄ derived from the observations of both SCIAMACHY and GOSAT. In the USA, NASA's Carbon Monitoring System is developing various projects to investigate carbon fluxes using satellite data and to create data products useful for researchers, policymakers and the private sector. In the UK, the National Centre for Earth Observation coordinates research into the creation and application of satellite data, including research focussed on the carbon cycle and climate.

Strategies and planning for satellite observations

Planning for new satellite missions is organised through national and regional programs such as ESA, NASA, and JAXA.

Corresponding expert groups, such as Copernicus and the US National Research Council, have provided advice to these programs on strategies for CO₂ and CH₄ emissions monitoring including satellite observations and other elements such as ground-based observations and bottom-up inventories^{5,69}.

Several international organisations also provide guidance on coordinating different types of observations and on ensuring continuity and cohesion between programs. The Group on Earth Observations (GEO) is a partnership of 100 countries providing conceptual and organisational guidance on Earth observation systems, including a strategy focused on carbon-related measurements⁷⁰. The Committee on Earth Observation Satellites, a collection of national agencies implementing satellite observations, has provided a detailed assessment of the new capabilities for carbon observations and the coordination of existing capabilities that are needed on an international level⁷¹. The World Meteorological Organization is also developing a strategy for an Integrated, Global Greenhouse Gas Information System (IG3IS).

Conclusion

Satellite observations provide valuable information about greenhouse gases and their emissions. Since the launch of SCIAMACHY on board Envisat in 2002, and more recently GOSAT and OCO-2, atmospheric column-averaged concentrations of the key greenhouse gases CO₂ and CH₄ have been measured remotely from space. These measurements are being used in flux inversions to provide estimates of natural fluxes of CO₂ and natural and anthropogenic fluxes of CH₄. Several strategies are being developed to use atmospheric CO₂ data for estimating fossil fuel CO₂ emissions, including the targeting of strong emitters such as megacities and the measurement of other gases that help to distinguish fossil fuel-derived CO₂.

Global land cover and forest biomass observations enable estimates of greenhouse gas emissions due to land use changes, including deforestation, that would not be possible using only ground-based surveys. Remote sensing of fires, night-time lights and biological activity provide the global coverage needed to calculate greenhouse gas emissions from fires, estimate the spatial distribution of energy consumption and detect large-scale patterns and trends in ecosystem productivity.

Planned future missions will extend current observational capabilities, allowing long-term trends to be investigated. Other missions will provide new and improved capabilities, and constellations of geostationary satellites offer the potential for improved observational coverage.

Satellite measurements provide unique opportunities to improve top-down and bottom-up estimation of greenhouse gas emissions, and satellites can be expected to provide key observations to support the monitoring and understanding of changes to the Earth's surface and atmosphere caused by human activities.

Further Information

Committee on Earth Observations Satellites
<http://ceos.org/>

EU Copernicus
<http://www.copernicus.eu/>

Global Climate Observing System
<http://www.wmo.int/pages/prog/gcos/>

Group on Earth Observations
<https://www.earthobservations.org/index.php>

NASA Carbon Monitoring System
<http://carbon.nasa.gov/>

National Centre for Earth Observation
<http://www.nceo.ac.uk/>

Satellite Applications Catapult
<https://sa.catapult.org.uk/>

List of Acronyms

AIRS – Atmospheric Infrared Sounder
AVHRR – Advanced Very High Resolution Radiometer
ESA – European Space Agency
FLEX – Fluorescence Explorer
GOSAT – Greenhouse Gas Observing Satellite
IASI – Infrared Atmospheric Sounding Interferometer
IPCC – Intergovernmental Panel on Climate Change
JAXA – Japan Aerospace Exploration Agency
LIDAR – Light Detection and Ranging
MODIS – Moderate Resolution Imaging Spectrometer
NASA – National Aeronautics and Space Administration (USA)
NDVI – Normalized Difference Vegetation Index
NIES – National Institute for Environmental Studies (Japan)
OCO-2 – Orbiting Carbon Observatory 2
SCIAMACHY – Scanning Imaging Absorption Spectrometer for Atmospheric Chartography
SEVIRI – Spinning Enhanced Visible and Infrared Imager
TANSO-CAI – Thermal and Near Infrared Sensor for Carbon Observation – Cloud and Aerosol Imager
TANSO-FTS – Thermal and Near Infrared Sensor for Carbon Observation – Fourier Transform Spectrometer
TCCON – Total Column Carbon Observing Network
TROPOMI – Tropospheric Monitoring Instrument
VIIRS – Visible Infrared Imaging Radiometer Suite

References

1. Hertzfeld, H. R. and R. A. Williamson (2007) The social and economic impact of Earth observing satellites, In: *Societal impact of spaceflight* [Dick, S. J. and R. D. Launius (eds.)], NASA, Washington DC.
2. IPCC (2013) Annex III: Glossary [Planton, S. (ed.)]. In: *Climate Change 2013: The Physical Science Basis. Contribution of Working Group I to the Fifth Assessment Report of the Intergovernmental Panel on Climate Change* [Stocker, T.F., D. Qin, G.-K. Plattner, M. Tignor, S.K. Allen, J. Boschung, A. Nauels, Y. Xia, V. Bex and P.M. Midgley (eds.)]. Cambridge University Press, Cambridge, United Kingdom and New York, NY, USA.
3. IPCC (2006) 2006 IPCC Guidelines for National Greenhouse Gas Inventories, Prepared by the National Greenhouse Gas Inventories Programme, Eggleston, H. S., Buendia L., Miwa K., Ngara T. and Tanabe K. (eds). Published: IGES, Japan.
4. Marquis, M. and Tans, P. (2008) Carbon Crucible, *Science*, 320, 460-461.
5. Pacala, S. W., C. Breidenich, P. G. Brewer, I. Fung, M. R. Gunson, G. Heddle, B. Law, G. Marland, K. Paustian, M. Prather, J. T. Randerson, P. Tans and S. C. Wofsy (2010) *Verifying Greenhouse Gas Emissions: Methods to Support International Climate Agreements*, National Academic Press, Washington DC, USA.
6. O'Brien, D. M. and P. J. Rayner (2002) Global observations of the carbon budget 2. CO₂ column from differential absorption of reflected sunlight in the 1.61 μm band of CO₂, *Journal of Geophysical Research*, 107 (D18), ACH 6-1 – ACH 6-16.
7. Kuang, Z., J. Margolis, G. Toon, D. Crisp, and Y. Yung (2002) Spaceborne measurements of atmospheric CO₂ by high-resolution NIR spectrometry of reflected sunlight: An introductory study, *Geophysical Research Letters*, 29, 1716, 11.
8. Duren, R. M. and C. E. Miller (2012) Measuring the carbon emissions of megacities, *Nature Climate Change*, 2, 560-562.
9. WMO/IAEA (2014) 17th WMO/IAEA Meeting on Carbon Dioxide, Other Greenhouse Gases and Related Tracers Measurement Techniques (GGMT-2013), GAW Report No. 213, World Meteorological Organization, Global Atmospheric Watch, July 2014.
10. Wunch, D., G. C. Toon, J.-F. L. Blavier, R. A. Washenfelder, J. Notholt, B. J. Connor, D. W. T. Griffith, V. Sherlock and P. O. Wennberg (2011) The Total Carbon Column Observing Network, *Phil. Trans. R. Soc. A*, 369, 2087-2112.
11. Parker, R., H. Boesch, A. Cogan, A. Fraser, L. Feng, P. I. Palmer, J. Messerschmidt, N. Deutscher, D. W. T. Griffith, J. Notholt, P. O. Wennberg and D. Wunch (2011) Methane observations from the Greenhouse Gases Observing SATellite: comparison to ground-based TCCON data and model calculations, *Geophysical Research Letters*, 38, L15807.
12. Washenfelder, R., Toon, G., Blavier, J.-F., Yang, Z., Allen, N., Wennberg, P., Vay, S., Matross, D., and Daube, B. (2006) Carbon dioxide column abundances at the Wisconsin Tall Tower site, *Journal of Geophysical Research*, 111, 1-11, doi:10.1029/2006JD007154.

13. Basu, S., S. Guerlet, A. Butz, S. Houweling, O. Hasekamp, I. Aben, P. Krummel, P. Steele, R. Langenfelds, M. Torn, S. Biraud, B. Stephens, A. Andrews and D. Worthy (2013) Global CO₂ fluxes estimated from GOSAT retrievals of total column CO₂, *Atmos. Chem. Phys.*, 13, 8695-8717.
14. Buchwitz, M., R. de Beek, J. P. Burrows, H. Bovensmann, T. Warneke, J. Notholt, J. F. Meirink, A. P. H. Goede, P. Bergamaschi, S. Körner, M. Heimann and A. Schulz (2005) Atmospheric methane and carbon dioxide from SCIAMACHY satellite data: initial comparison with chemistry and transport models, *Atmos. Chem. Phys.*, 5, 941-962.
15. Yokota, T., Y. Yoshida, N. Eguchi, Y. Ota, T. Tanaka, H. Watanabe, and S. Maksyutov (2009) Global Concentrations of CO₂ and CH₄ Retrieved from GOSAT: First Preliminary Results, *SOLA*, 5, 160-163.
16. ESA (2015) *Report for Mission Selection: CarbonSat*, ESA SP-1330/1 (2 volume series), European Space Agency, Noordwijk, The Netherlands.
17. Buchwitz, M., H. Bovensmann, J. P. Burrows, O. Schneising and M. Reuter (2010) *Global mapping of methane and carbon dioxide: from SCIAMACHY to CarbonSat*, In: *Proceedings ESA-iLEAPS-EGU conference on earth observation for land-atmosphere interaction science*, ESA Special Publications SP-688, ESRI, Italy, 3-5 Nov 2010.
18. Houweling, S., D. Baker, S. Basu, H. Boesch, A. Butz, F. Chevallier, F. Deng, E. J. Dlugokencky, L. Feng, A. Ganshin, O. Hasekamp, D. Jones, S. Maksyutov, J. Marshall, T. Oda, C. W. O'Dell, S. Oshchepkov, P. I. Palmer, P. Peylin, Z. Poussi, F. Reum, H. Takagi, Y. Yoshida and R. Zhuravlev (2015) An intercomparison of inverse models for estimating sources and sinks of CO₂ using GOSAT measurements. *J. Geophys. Res. Atmos.*, 120, 5253-5266. doi: 10.1002/2014JD022962.
19. Gurney, K. R., R. M. Law, A. S. Denning, P. J. Rayner, D. Baker, P. Bousquet, L. Bruhwiler, Y.-H. Chen, P. Ciais, S. Fan, I. Y. Fung, M. Gloor, M. Heimann, K. Higuchi, J. John, T. Maki, S. Maksyutov, K. Masarie, P. Peylin, M. Prater, B. C. Pak, J. Randerson, J. Sarmiento, S. Taguchi, T. Takahashi and C.-W. Yuen (2002) Towards robust regional estimates of CO₂ sources and sinks using atmospheric transport models, *Nature*, 415, 626-630.
20. Niwa, Y., T. Machida, Y. Sawa, H. Matsueda, T. J. Schuck, C. A. M. Brenninkmeijer, R. Imasu and M. Satoh (2012) Imposing strong constraints on tropical terrestrial CO₂ fluxes using passenger aircraft based measurements. *Journal of Geophysical Research: Atmospheres*, 117(D11), D11303. doi:10.1029/2012JD017474
21. Turner, A. J., D. J. Jacob, K. J. Wecht, J. D. Massakkers, E. Lundgren, A. E. Andrews, S. C. Biraud, H. Boesch, K. W. Bowman, N. M. Deutscher, M. K. Dubey, D. W. T. Griffith, F. Hase, A. Kuze, J. Notholt, H. Ohyama, R. Parker, V. H. Payne, R. Sussman, C. Sweeney, V. A. Velazco, T. Warneke, P. O. Wennberg and D. Wunch (2015) Estimating global and North American methane emissions with high spatial resolution using GOSAT satellite data, *Atmos. Chem. Phys.*, 15, 7049-7069.
22. UN (2015) *World Urbanization Prospects: The 2014 Revision*, (ST/ESA/SER.A/366). United Nations Department of Economic and Social Affairs, Population Division.
23. Velazco, V. A., M. Buchwitz, H. Bovensmann, M. Reuter, O. Schneising, J. Heymann, T. Krings, K. Gerilowski, J. P. Burrows (2011) Towards space based verification of CO₂ emissions from strong localized sources: fossil fuel power plant emissions as seen by a CarbonSat constellation, *Atmos. Meas. Tech.*, 4, 2809-2822.
24. Kort, E. A., C. Frankenberg, C. E. Miller and T. Oda (2012) Space-based observations of megacity carbon dioxide, *Geophysical Research Letters*, 39, L17806.
25. Berezin, E. V., I. B. Konovalov, P. Ciais, A. Richter, S. Tao, G. Janssens-Maenhout, M. Beekmann and E.-D. Schulze (2013) Multiannual changes of CO₂ emissions in China: indirect estimates derived from satellite measurements of tropospheric NO₂ columns, *Atmos. Chem. Phys.*, 13, 9415-9438.
26. Reuter, M., M. Buchwitz, A. Hilboll, A. Richter, O. Schneising, M. Hilker, J. Heymann, H. Bovensmann and J. P. Burrows (2014) Decreasing emissions of NO_x relative to CO₂ in East Asia inferred from satellite observations, *Nature Geoscience*, 7, 792-795.
27. Levin, I., B. Kromer, M. Schmidt and H. Sartorius (2003) A novel approach for independent budgeting of fossil fuel CO₂ over Europe by 14CO₂ observations, *Geophysical Research Letters*, 30, 2194.
28. Megacities Carbon Project (2014) *Megacities Carbon Project* [Online] Available at: <https://megacities.jpl.nasa.gov/portal> [Accessed: 07/09/2015]
29. Kirschke, S., P. Bousquet, P. Ciais, M. Saunoy, J. G. Canadell, E. J. Dlugokencky, P. Bergamaschi, D. Bergmann, D. R. Blake, L. Bruhwiler, P. Cameron-Smith, S. Castaldi, F. Chevallier, L. Feng, A. Fraser, M. Heimann, E. L. Hodson, S. Houweling, B. Josse, P. J. Fraser, P. B. Krummel, J.-F. Lamarque, R. L. Langenfelds, C. Le Quééré, V. Naik, S. O'Doherty, P. I. Palmer, I. Pison, D. Plummer, B. Poulter, R. G. Prinn, M. Rigby, B. Ringeval, M. Santini, M. Schmidt, D. T. Shindell, I. J. Simpson, R. Spahni, L. P. Steele, S. A. Strode, K. Sudo, S. Szopa, G. R. van der Werf, A. Voulgarakis, M. van Weele, R. F. Weiss, J. E. Williams and G. Zeng (2013) Three decades of global methane sources and sinks, *Nature geoscience*, 6, 813-823.
30. Wecht, K. J., D. J. Jacob, C. Frankenberg, Z. Jiang and D. R. Blake (2014) Mapping of North American methane emissions with high spatial resolution by inversion of SCIAMACHY satellite data, *Journal of Geophysical Research – Atmospheres*, 119, 7741-7756.
31. Kort, E. A., C. Frankenberg, K. R. Costigan, R. Lindenmaier, M. K. Dubey and D. Wunch (2014) Four corners: The largest US methane anomaly viewed from space, *Geophysical Research Letters*, 41, 6898-6903.
32. Bergamaschi, P., M. Corazza, U. Karstens, M. Athanassiadou, R. L. Thompson, I. Pison, A. J. Manning, P. Bousquet, A. Segers, A. T. Vermeulen, G. Janssens-Maenhout, M. Schmidt, M. Ramonet, F. Meinhardt, T. Aalto, L. Haszpra, J. Moncrieff, M. E. Popa, D. Lowry, M. Steinbacher, A. Jordan, S. O'Doherty, S. Piacentino and E. Dlugokencky (2015) Top-down estimates of European CH₄ and N₂O emissions based on four different inverse models, *Atmos. Chem. Phys.*, 15, 715-736.
33. Liu, Y., D. Yang and Z. Cai (2013) A retrieval algorithm for TanSat XCO₂ observation: Retrieval experiments using GOSAT data, *Chinese Science Bulletin*, 58, 1520-1523.
34. Bi, Y., Z. Yang, S. Gu, Q. Wang, L. Gao and J. Chen (2014) Impacts of aerosol and albedo on TanSat CO₂ retrieval using the near infrared CO₂ bands, *Remote Sensing of the Atmosphere, Clouds and Precipitation V* [Eds: E. Im, S. Yang and P. Zhang], Proc. Of SPIE, 925915.
35. GHGSat (2015) GHGSat, [Online] Available from: <http://www.ghgsat.com>, [Accessed 13/10/2015]
36. National Institute for Environmental Studies (NIES) (2015) *About the GOSAT-2 Mission*, [Online] Available from: <http://www.gosat-2.nies.go.jp/about/mission/> [Accessed: 22/09/2015]

37. Glumb, R. J., C. Lietzke, J. Bougher, A. D. Bell and C. Ellsworth (2015) The TANSO-FTS Instrument for the GOSAT-2 Greenhouse Gas Monitoring Mission, *20th Conference on Satellite Meteorology and Oceanography*, Phoenix, Arizona, USA.
38. Schneising, O., J. Heymann, M. Buchwitz, M. Reuter, H. Bovensmann and J. P. Burrows (2013) Anthropogenic carbon dioxide source areas observed from space: assessment of regional enhancements and trends, *Atmos. Chem. Phys.*, **13**, 2445-2454.
39. Buchwitz, M., M. Reuter, H. Bovensmann, D. Pillai, J. Heymann, O. Schneising, V. Rozanov, T. Krings, J. P. Burrows, H. Boesch, C. Gerbig, Y. Meijer and A. Löscher (2013) Carbon Monitoring Satellite (CarbonSat): assessment of atmospheric CO₂ and CH₄ retrieval errors by error parameterization, *Atmos. Meas. Tech.*, **6**, 3477-3500.
40. Abshire, J. B., H. Riris, G. R. Allan, C. J. Weaver, J. Mao, X. Sun, W. E. Hasselbrack, S. R. Kawa and S. Biraud (2010) Pulsed airborne lidar measurements of atmospheric CO₂ column absorption, *Tellus*, **628**, 770-783.
41. Hansen, M. C., P. V. Potapov, R. Moore, M. Hancher, S. A. Turubanova, A. Tyukavina, D. Thau, S. V. Stehman, S. J. Goetz, T. R. Loveland, A. Kommareddy, A. Egorov, L. Chini, C. O. Justice and J. R. G. Townshend (2013) High-resolution global maps of 21st-century forest cover change, *Science*, **342**, 850-853.
42. Kim, D.-H., J. O. Sexton and J. R. Townshend (2015) Accelerated deforestation in the humid tropics from the 1990s to the 2000s, *Geophysical Research Letters*, **42**, 3495-3501.
43. Abshire, J. B., X. Sun, H. Riris, J. M. Sirota, J. F. McGarry, S. Palm, D. Yi and P. Liiva (2005) Geoscience Laser Altimeter System (GLAS) on the ICESat Mission: On-orbit measurement performance, *Geophysical Research Letters*, **32**, L21S02.
44. Saatchi, S. S., N. L. Harris, S. Brown, M. Lefsky, E. T. A. Mitchard, W. Salas, B. R. Zutta, W. Buermann, S. L. Lewis, S. Hagen, S. Petrova, L. White, M. Silman and A. Morel (2011) Benchmark map of forest carbon stocks in tropical regions across three continents, *PNAS*, **108**, 9899-9904.
45. Harris, N. L., S. Brown, S. C. Hagen, S. S. Saatchi, S. Petrova, W. Salas, M. C. Hansen, P. V. Potapov and A. Lotsch (2012) Baseline map of carbon emissions from deforestation in tropical regions, *Science*, **336**, 1573.
46. Achard, F., R. Beuchle, P. Mayaux, H.-J. Stibig, C. Bodart, A. Brink, S. Carboni, B. Desclée, F. Donnay, H. D. Eva, A. Lupi, R. Raši, R. Seliger and D. Simonetti (2014) Determination of tropical deforestation rates and related carbon losses from 1990 to 2010, *Global Change Biology*, **20**, 2540-2554.
47. Song, X. P., C. Q. Huang, S. S. Saatchi, M. C. Hansen and J. R. Townshend (2015) Annual carbon emissions from deforestation in the Amazon basin between 2000 and 2010, *PLoS One*, **10**, doi:10.1371/journal.pone.0126754
48. Giglio, L., J. Descloitres, C. O. Justice and Y. J. Kaufman (2003) An enhanced contextual fire detection algorithm for MODIS, *Remote Sensing of Environment*, **87**, 273-282.
49. Schroeder, W., P. Oliva, L. Giglio and I. Csizsar (2014) The new VIIRS 375 m active fire detection data product: Algorithm description and initial assessment, *Remote Sensing of Environment*, **143**, 85-96.
50. Boles, S. H. and D. L. Verbyla (2000) Comparison of three AVHRR-based fire detection algorithms for interior Alaska, *Remote Sensing of Environment*, **1**, 1-16.
51. Roberts, G. J. and M. J. Wooster (2008) Fire detection and fire characterization over Africa using Meteosat SEVIRI, *IEEE Transactions on Geoscience and Remote Sensing*, **46**, 1200-1218.
52. Schroeder, W., P. Oliva, L. Giglio, B. Quayle, E. Lorenz and F. Morelli (2015) Active fire detection using Landsat-8/OLI data, *Remote Sensing of Environment*, doi:10.1016/j.rse.2015.08.032.
53. Roy, D. P., Y. Jin, P. E. Lewis and C. O. Justice (2005) Prototyping a global algorithm for systematic fire-affected area mapping using MODIS time series data, *Remote Sensing of Environment*, **97**, 137-162.
54. Van der Werf, G. R., J. T. Randerson, L. Giglio, G. J. Collatz, M. Mu, P. S. Kasibhatla, D. C. Morton, R. S. DeFries, Y. Jin and T. T. van Leeuwen (2010) Global fire emissions and the contribution of deforestation, savannah, forest, agricultural, and peat fires (1997-2009), *Atmos. Chem. Phys.*, **10**, 11707-11735.
55. Boden, T.A., G. Marland, and R.J. Andres. 2015. Global, Regional, and National Fossil-Fuel CO₂ Emissions. Carbon Dioxide Information Analysis Center, Oak Ridge National Laboratory, U.S. Department of Energy, Oak Ridge, Tenn., U.S.A. doi 10.3334/CDIAC/00001_V2015.
56. Oda, T. and S. Maksyutov (2011) A very high-resolution (1 kmx1 km) global fossil fuel CO₂ emission inventory derived using a point source database and satellite observations of nighttime lights, *Atmos. Chem. Phys.*, **11**, 543-556.
57. Asefi-Najafabady, S., P. J. Rayner, K. R. Gurney, A. McRobert, Y. Song, K. Coltin, J. Huang, C. Elvidge and K. Baugh (2014) A multiyear, global gridded fossil fuel CO₂ emission data product: Evaluation and analysis of results, *Journal of Geophysical Research: Atmospheres*, **10**, 213-10231.
58. Myneni, R. B., S. Hoffman, Y. Knyazikhin, J. L. Privette, J. Glassy, Y. Tian, Y. Wang, X. Song, Y. Zhang, G. R. Smith, A. Lotsch, M. Friedl, J. T. Morisette, P. Votava, R. R. Nemani and S. W. Running (2002) Global products of vegetation leaf area and fraction absorbed PAR from year one of MODIS data, *Remote Sensing of Environment*, **83**, 214-231.
59. Donohue, R. J., M. L. Roderick and T. R. McVicar (2008) Deriving consistent long-term vegetation information from AVHRR reflectance data using a cover-triangle-based framework, *Remote Sensing of Environment*, **112**, 2938-2949.
60. Pickett-Heaps, C. A., J. G. Canadell, P. R. Briggs, N. Gobron, V. Haverd, M. J. Paget, B. Pinty and M. R. Raupach (2014) Evaluation of six satellite-derived Fraction of Absorbed Photosynthetic Active Radiation (FAPAR) products across the Australian continent, *Remote Sensing of Environment*, **140**, 241-256.
61. O'Reilly, J. E., S. Maritorena, B. G. Mitchell, D. A. Siegel, K. L. Carder, S. A. Garver, M. Kahru and C. McClain (1998) Ocean color chlorophyll algorithms for SeaWiFS, *Journal of Geophysical Research*, **103**, C11, 24937-24953.
62. Nemani, R. R., C. D. Keeling, H. Hashimoto, W. M. Jolly, S. C. Piper, C. J. Tucker, R. B. Myneni and S. W. Running (2003) Climate-driven increases in global terrestrial net primary production from 1982 to 1999, *Science*, **300**(5625), 1560-1563.
63. Behrenfeld, M. J., R. T. O'Malley, D. A. Siegel, C. R. McClain, J. L. Sarmiento, G. C. Feldman, A. J. Milligan, P. G. Falkowski, R. M. Letelier and E. S. Boss (2006) Climate-driven trends in contemporary ocean productivity, *Nature*, **444**(7120), 752-755.

64. Frankenberg, C., C. O'Dell, J. Berry, L. Guanter, J. Joiner, P. Kohler, R. Pollock and T. E. Taylor (2014) Prospects for chlorophyll fluorescence remote sensing from Orbiting Carbon Observatory-2, *Remote Sensing of Environment*, 147, 1-12.
65. Joiner, J., Y. Yoshida, A. P. Vasilkov, Y. Yoshida, L. A. Corp and E. M. Middleton (2011) First observations of global and seasonal terrestrial chlorophyll fluorescence from space, *Biogeosciences*, 8, 637-651.
66. Ramsayer, K. and S. Cole (2015) The Landsat Mission Continues [Online] Available from: <http://landsat.gsfc.nasa.gov/?p=10391> [Accessed 15/10/2015]
67. ESA (2012) *Report for mission selection: Biomass*, ESA SP-1324/1 (3 volume series), European Space Agency, Noordwijk, The Netherlands.
68. Kraft, S, U. Del Bello, M. Bouvet, M. Drusch and J. Moreno (2012) FLEX: ESA's Earth Explorer 8 candidate mission, *Geoscience and Remote Sensing Symposium (IGARSS)*, IEEE International.
69. Ciais, P., D. Crisp, H. D. van der Gon, R. Engelen, G. Janssens-Maenhout, M. Heimann, P. Rayner and M. Scholze (2015) *Towards a European Operational Observing System to Monitor Fossil CO₂ Emissions: Report from the expert group*. European Commission, Brussels.
70. Ciais, P., A. J. Dolman, R. Dargaville, L. Barrie, A. Bombelli, J. Butler, P. Canadell, and T. Moriyama (2010) *Geo Carbon Strategy*, Geo Secretariat Geneva, FAO, Rome, 48 pp.
71. CEOS (2014) *CEOS Strategy for Carbon Observations from Space*. The Committee on Earth Observation Satellites (CEOS) Response to the Group on Earth Observations (GEO) Carbon Strategy. September 30 2014.

About the authors

Dr Stephen Hardwick is a postdoctoral researcher in the Department of Physics at Imperial College London. He has a PhD from the Grantham Institute in atmospheric physics and tropical ecology. His research focuses on the impacts of climate change and interactions between the climate system and the biosphere.

Dr Heather Graven is a Lecturer in the Department of Physics and the Grantham Institute at Imperial College London. She studied for her PhD at Scripps Institution of Oceanography, USA and worked previously at ETH Zurich, Switzerland. Her research focuses on the use of atmospheric measurements to understand the global carbon cycle and its response to human activities and climate change.

About the Grantham Institute

The Grantham Institute is committed to driving research on climate change and the environment, and translating it into real world impact. Established in February 2007 with a £12.8 million donation over ten years from the Grantham Foundation for the Protection of the Environment, the Institute's researchers are developing both the fundamental scientific understanding of climate and environmental change, and the mitigation and adaptation responses to it. The research, policy and outreach work that the Institute carries out is based on, and backed up by, the worldleading research by academic staff at Imperial.

www.imperial.ac.uk/grantham

About Imperial College London

Consistently rated amongst the world's best universities, Imperial College London is a science-based institution with a reputation for excellence in teaching and research that attracts 13,000 students and 6,000 staff of the highest international quality.

Innovative research at the College explores the interface between science, medicine, engineering and business, delivering practical solutions that improve quality of life and the environment—underpinned by a dynamic enterprise culture. Since its foundation in 1907, Imperial's contributions to society have included the discovery of penicillin, the development of holography and the foundations of fibre optics.

This commitment to the application of research for the benefit of all continues today, with current focuses including interdisciplinary collaborations to improve health in the UK and globally, tackle climate change and develop clean and sustainable sources of energy.

www.imperial.ac.uk



This is **naturally responsible** Printing

virtually **Zero** waste

100%	100%	100%	100%	100%	100%
carbon neutral	EMAS	renewable energy	ISO14001	eco-friendly simitri® toner	recycled FSC stock

printed by **seacourt** proud to be counted amongst the top environmental printers in the world www.seacourt.net